



ISSN 0264-4401  
Volume 00 Number 00 2018

**Engineering Computations**

International journal for computer-aided  
engineering and software



**An evolutionary modelling approach to predicting stress-strain behaviour of saturated granular soils**

Journal:	<i>Engineering Computations</i>
Manuscript ID	EC-01-2018-0025.R3
Manuscript Type:	Research Article
Keywords:	granular soils, triaxial stress-strain behaviour, evolutionary-based data mining

SCHOLARONE™  
Manuscripts

## An evolutionary modelling approach to predicting stress-strain behaviour of saturated granular soils

### Abstract

**Purpose** - To develop a unified framework for modelling triaxial deviator stress - axial strain and volumetric strain – axial strain behaviour of granular soils with the ability to predict the entire stress paths, incrementally, point by point, in deviator stress versus axial strain, and volumetric strain versus axial strain spaces using an evolutionary-based technique based on a comprehensive set of data directly measured from triaxial tests without pre-processing. 177 triaxial test results acquired from literature were used to develop and validate the models. Models aimed not only to be capable of capturing and generalising the complicated behaviour of soils but also to explicitly remain consistent with expert knowledge available for such behaviour.

**Methodology** - Evolutionary polynomial regression was used to develop models to predict stress - axial strain and volumetric strain – axial strain behaviour of granular soils. EPR integrates numerical and symbolic regression to perform evolutionary polynomial regression. The strategy uses polynomial structures to take advantage of favourable mathematical properties. EPR is a two-stage technique for constructing symbolic models. It initially implements evolutionary search for exponents of polynomial expressions using a genetic algorithm (GA) engine to find the best form of function structure, secondly it performs a least squares regression to find adjustable parameters, for each combination of inputs (terms in the polynomial structure).

**Findings** - EPR-based models were capable of generalizing the training to predict the behaviour of granular soils under conditions that have not been previously seen by EPR in the training stage. It was shown that the proposed EPR models outperformed ANN and provided closer predictions to the experimental data cases. The entire stress paths for the shearing

1  
2  
3 behaviour of granular soils using developed model predictions were created with very good  
4 accuracy despite error accumulation. Parametric study results revealed the consistency of  
5 developed model predictions, considering roles of various contributing parameters, with  
6 physical and engineering understandings of the shearing behaviour of granular soils.  
7  
8  
9

10  
11 **Originality/value** - In this paper, an evolutionary-based data-mining method was  
12 implemented to develop a novel unified framework to model the complicated stress-strain  
13 behaviour of saturated granular soils. The proposed methodology overcomes the drawbacks  
14 of artificial neural network-based models with black box nature by developing accurate,  
15 explicit, structured and user-friendly polynomial models, and enabling the expert user to  
16 obtain a clear understanding of the system.  
17  
18  
19  
20  
21  
22  
23  
24  
25

## 26 **Introduction**

27  
28 The shear strength of cohesionless soil such as sand and gravel under varying drainage  
29 conditions has been a topic of significant interest for the last four decades. Many research  
30 works have contributed significantly to understanding of the important factors that control the  
31 shear strength behaviour of sand and gravel in drained conditions, including large number of  
32 experiments e.g. triaxial tests conducted with results published in the literature. There has  
33 been a lot of interest in the research community to model the shear stress and volume change  
34 behaviour of cohesionless soil and because of its well defined conditions of stress and strain  
35 on the cylindrical specimens, many of the models developed to date are predominantly based  
36 on triaxial compression test data. The majority of the past research effort has been devoted to  
37 modelling of soil behaviour using the elasticity/plasticity based approach with some success  
38 (Rowe and Barden 1964). Ellis et al (1995) suggested a feed-back neural network model for  
39 representing shearing behaviour of sand in undrained conditions. Following Ellis et al (1995)  
40 work, Penumadu and Zhao (1999) also developed a neural network based models for triaxial  
41  
42  
43  
44  
45  
46  
47  
48  
49  
50  
51  
52  
53  
54  
55  
56  
57  
58  
59  
60

1  
2  
3 compression behaviour of sand and gravel. The results presented in their paper, representing  
4 the deviator stress and volume change behaviour of varying types of sand and gravel for  
5 drained conditions, suggested some improvements compared to Ellis et al (1995) work  
6  
7 (Penumadu and Zhao 1999): (i) developing a suitable strain increment value in the feed-back  
8  
9 process; (ii) avoiding errors associated with over-training during the training phase; (iii)  
10  
11 implementing a procedure for obtaining optimal size of the hidden layer; and (iv) modelling  
12  
13 triaxial compression behaviour of both sand and gravel under drained conditions. In this  
14  
15 research work the evolutionary polynomial regression (EPR) is implemented to develop  
16  
17 structured and transparent models in the form of polynomial equations to represent the shear  
18  
19 strength and volume change behaviour of saturated granular geomaterials. EPR models have  
20  
21 the capability of capturing and representing the behaviour of materials in easily  
22  
23 understandable form for the user. A clear insight into the role of different contributing  
24  
25 parameters is also given to the users by the developed models helping them better understand  
26  
27 the physics of complicated behaviour of materials and systems.  
28  
29  
30  
31

32  
33 A comprehensive set of data from literature was collected and used to develop and validate  
34  
35 the EPR models for stress-strain and volume change behaviour of cohesionless soils.  
36

37 Data preparation, model development procedure and also the merits and advantages of the  
38  
39 proposed technique will be discussed in detail in following sections in this paper.  
40  
41 Comparisons are also made between EPR model predictions and the experimental data as  
42  
43 well as results from artificial neural network model predictions presented by Penumadu and  
44  
45 Zhao (1999). Sensitivity analysis outcomes and the relevant discussions are also presented in  
46  
47 next coming parts of paper.  
48  
49

## 50 **Evolutionary Polynomial Regression**

51  
52 Evolutionary polynomial regression EPR integrates numerical and symbolic regression to  
53  
54 perform evolutionary polynomial regression. The strategy uses polynomial structures to take  
55  
56  
57  
58  
59  
60

1  
2  
3 advantage of their favourable mathematical properties. The key idea behind the EPR is to use  
4  
5 evolutionary search for exponents of polynomial expressions by means of a genetic algorithm  
6  
7 (GA) engine. This allows (i) easy computational implementation of the algorithm, (ii)  
8  
9 efficient search for an explicit expression, and (iii) improved control of the complexity of the  
10  
11 expression generated (Giustolisi and Savic 2006). EPR is a data-driven method based on  
12  
13 evolutionary computing, aimed to search for polynomial structures representing a system. A  
14  
15 physical system, having an output  $y$ , dependent on a set of inputs  $X$  and parameters  $\theta$ , can be  
16  
17 mathematically formulated as:

$$20 \quad y = F(\mathbf{X}, \boldsymbol{\theta}) \quad (1)$$

21  
22 where  $F$  is a function in an  $m$ -dimensional space and  $m$  is the number of inputs. To avoid the  
23  
24 problem of mathematical expressions growing rapidly in length with time, in EPR the  
25  
26 evolutionary procedure is conducted in the way that it searches for the exponents of a  
27  
28 polynomial function with a fixed maximum number of terms. During one execution it returns  
29  
30 a number of expressions with increasing numbers of terms up to a limit set by the user, to  
31  
32 allow the optimum number of terms to be selected. The general form of expression used in  
33  
34 EPR can be presented as (Giustolisi and Savic 2006):

$$35 \quad y = \sum_{j=1}^m F(\mathbf{X}, f(\mathbf{X}), a_j) + a_0 \quad (2)$$

36  
37 where  $y$  is the estimated vector of output of the process;  $a_j$  is a constant;  $F$  is a function  
38  
39 constructed by the process;  $X$  is the matrix of input variables;  $f$  is a function defined by the  
40  
41 user (it may be natural logarithmic, exponential, tangent hyperbolic, etc.); and  $m$  is the  
42  
43 number of terms of the target expression. The first step in identification of the model  
44  
45 structure is to transfer Equation 2 into the following vector form:

$$46 \quad Y_{N \times 1}(\theta, Z) = \begin{bmatrix} I_{N \times 1} & Z_{N \times m}^j \end{bmatrix} \times [a_0 \quad a_1 \quad \dots \quad a_m]^T = Z_{N \times d} \times \theta_{d \times 1}^T \quad (3)$$

where  $Y_{N \times 1}(\theta, Z)$  is the least squares estimate vector of the  $N$  target values;  $\theta_{d \times 1}$  is the vector of  $d=m+1$  parameters  $a_j$  and  $a_0$  ( $\theta^T$  is the transposed vector); and  $Z_{N \times d}$  is a matrix formed by  $I$  (unitary vector) for bias  $a_0$ , and  $m$  vectors of variables  $Z_j$ . For a fixed  $j$ , the variables  $Z_j$  are a product of the independent predictor vectors of inputs,  $X = \langle X_1 X_2 \dots X_k \rangle$  (where “ $k$ ” is the number of independent predictor variables – inputs).  $Z_j$  is a transformed variable which is a function of the independent variables,  $X_1 X_2 \dots X_k$ , evaluated at the  $j^{\text{th}}$  data point (Giustolisi and Savic 2006).

In general, EPR is a two-stage technique for constructing symbolic models. Initially, using standard genetic algorithm (GA), it searches for the best form of the function structure, i.e. a combination of vectors of independent inputs,  $X_s=1:k$  (where “ $k$ ” is the number of independent predictor variables – inputs), and secondly it performs a least squares regression to find the adjustable parameters,  $\theta$ , for each combination of inputs. In this way a global search algorithm is implemented for both the best set of input combinations and related exponents simultaneously, according to the user-defined cost function (Giustolisi and Savic 2006). The adjustable parameters,  $a_j$ , are evaluated by means of the linear least squares (LS) method based on minimization of the sum of squared errors (SSE) as the cost function. The SSE function which is used to guide the search process towards the best fit model is as follows:

$$\text{SSE} = \frac{\sum_{i=1}^N (y_a - y_p)^2}{N} \quad (4)$$

where  $y_a$  and  $y_p$  are the target experimental and the model prediction values respectively. The global search for the best form of the EPR equation is performed by means of a standard GA over the values in the user defined vector of exponents. The GA operates based on Darwinian evolution which begins with random creation of an initial population of solutions. Each parameter set in the population represents the individual’s chromosomes. Each

1  
2  
3 individual is assigned a fitness based on how well it performs in its environment. Through  
4 crossover and mutation operations, with the probabilities  $P_c$  and  $P_m$  respectively, the next  
5 generation is created. Fit individuals are selected for mating, whereas weak individuals die  
6 off. The mated parents create a child (offspring) with a chromosome set which is a mix of  
7 parents' chromosomes. In EPR integer GA coding with single point crossover is used to  
8 determine the location of the candidate exponents.

9  
10  
11 The EPR process stops when the termination criterion, which can be either the maximum  
12 number of generations, the maximum number of terms in the target mathematical expression  
13 or a particular allowable error, is satisfied. A typical flow diagram for the EPR procedure is  
14 illustrated in Figure 1.

### 15 **Database and the parameters involved in development of the models**

16  
17 Previous experimental research has shown that the important factors that govern the  
18 behaviour of cohesionless soils (sand and gravel) are their mineralogy, particle shape, particle  
19 size and its distribution, void ratio and also the effective confining stress level (Penumadu  
20 and Zhao 1999). The experimental database from a large number of contributions from  
21 literature (Table 1) was used to develop the models in this research. The database included  
22 the effects of the above mentioned factors systematically in a comprehensive manner using a  
23 large number of drained triaxial compression tests.

24  
25 The objective was to develop EPR-based models to represent the deviator stress-axial strain,  
26 and volumetric strain-axial strain relationships for granular soils with varying mineralogy,  
27 particle shape, uniformity coefficient, coefficient of curvature, effective particle size, void  
28 ratio, and effective confining pressure.

29  
30 Data from a total of 177 triaxial compression tests were obtained from literature. Using the  
31 approach proposed by Hardin (1985), the mineralogy and grain shape were quantified in the  
32 database using crushing hardness, and average particle shape factor. The crushing hardness,  $h$

(a mineralogy factor) is approximately equal to the scratch hardness as defined by Moh's Scale. It takes a value of 7, 6, and 3 for quartz, feldspar, and calcite respectively. The shape factor ( $n_s$ ) defines the degree of angularity, and is equal to: 25 for angular, 20 for sub-angular, 17 for sub-round, and 15 for round shape (Penumadu and Zhao 1999).

## Data preparation

From among 177 triaxial test results, 138 (80%) was used for model construction and the remaining 39 (20%), kept unseen to EPR during the model development procedure, was implemented to validate the developed models. It was checked to make sure that all parameter values in the testing data sets were within the range of data chosen to be used for training EPR and developing the models to avoid extrapolation.

To select the most robust combination of the training and testing data, a statistical analysis was performed on the input and output parameter values (Table 2) of several randomly selected training and validation data combinations. The aim of the analysis was to ensure that the statistical properties of the data in each of the subsets (training or testing) were as close to the other as possible and thus represented the same statistical population. The mean and standard deviation values were calculated for every single contributing parameter and for the training and testing datasets for every randomly considered combination and the combination for which these statistical values were the closest in the training and testing data sets was chosen to be used in training and testing stages in the EPR model development process (Hussain M. S. 2015, Ahangar Asr and Javadi 2016).

## EPR Procedure

Before starting the evolutionary procedure, a number of constraints can be implemented to control the structure of the models to be constructed, in terms of type of functions used, number of terms, range of exponents, number of generations etc. It can be seen that there is a potential to achieve different models for a particular problem which enables the user to gain



additional information (Javadi and Rezanian 2009). Applying the EPR procedure, the evolutionary process starts from a constant mean of output values. By increasing the number of evolutions it gradually picks up the different participating parameters in order to form equations representing the relationship between contributing and output parameters. Each model is trained using the training data and tested using the testing data. The level of accuracy at each stage is evaluated based on the coefficient of determination (COD) i.e. the fitness function:

$$\text{COD} = 1 - \frac{\sum_N (\mathbf{Y}_a - \mathbf{Y}_p)^2}{\sum_N \left( \mathbf{Y}_a - \frac{1}{N} \sum_N \mathbf{Y}_a \right)^2} \quad (5)$$

where  $\mathbf{Y}_a$  is the actual output value;  $\mathbf{Y}_p$  is the EPR predicted value and  $N$  is the number of data points on which the COD is computed. If the model fitness is not acceptable or the other termination criteria (in terms of maximum number of generations and maximum number of terms) are not satisfied, the current model should go through another evolution in order to obtain a new model.

### Developing the EPR models

A typical scheme to train most of the neural network based material models for soils includes an input set providing the network with information relating to the current state units (e.g., current stresses and strains) and then a forward pass through the network yields the prediction of the next expected state of stress or strain relevant to an input strain or stress increment (Ghaboussi, et al. 1998); (Penumadu and Zhao 1999)). Due to the incremental nature of soil stress-strain modelling in practical applications, the same scheme was also used in this research to model the behaviour of granular materials.

The EPR models had 11 input parameters (Table 2).  $D_{50}$ ,  $C_u$ ,  $C_c$ ,  $h$ ,  $n_s$ ,  $e$  and  $\sigma_3$  represented the initial conditions of the soil specimens, but the other three parameters, namely axial strain, volumetric strain, and deviator stress were updated incrementally during the training and

testing based on the outputs from the previous increment of the axial strain. The output parameters were the deviator stress and the volumetric strain corresponding to the end of the incremental step and were calculated using the two EPR models.

The training of the EPR resulted in development of more than one equation for deviator stress. From among the EPR outcome equations, 2 did not include the effect of all contributing parameters meaning that that the introduced parameters to EPR were not appearing in the resulted models. From the remaining equations with all the desired parameters involved, the most appropriate and efficient one based on the: (i) model performance (fitness); (ii) complexity; and also (iii) the sensitivity analysis results was chosen as the final model. A similar procedure was also followed to create and choose the best equation (model) for the volumetric behaviour. Equations 6 and 7 represent the EPR models for deviator stress and volume strain respectively.

$$q_{i+1} = -\frac{1.3E(-5)C_c^3 \varepsilon_a \Delta \varepsilon_a \sigma_3 \varepsilon_{v_i}}{D_{50}^2 C_u^3} + \frac{1.1E(-4)C_c^3 h^3 n_s^3 \varepsilon_a \Delta \varepsilon_a}{D_{50} C_u e^3 q_i} + \frac{0.1n_s^3 \Delta \varepsilon_a}{C_u C_c^2 h e^2} + \frac{0.2C_c h \Delta \varepsilon_a \sigma_3}{n_s} \\ + \frac{60.9C_u \Delta \varepsilon_a \sigma_3 \varepsilon_{v_i}}{C_c^2 n_s^2 q_i} + \frac{2.3E(-9)C_u^3 e^3 \sigma_3^3 \varepsilon_{v_i}}{C_c^2 h^2 n_s^3 \Delta \varepsilon_a^2} + \frac{2.3E(-4)C_u^3 \Delta \varepsilon_a^2 \sigma_3^2 \varepsilon_{v_i}}{h^2 n_s^2 q_i} \\ + \frac{5.9E(-4)D_{50} C_c^3 e^2 \sigma_3^3 \varepsilon_{v_i}^2}{C_u^2 h n_s^3 \Delta \varepsilon_a q_i} + \frac{8.3E(-9)D_{50} h^3 \varepsilon_a \Delta \varepsilon_a^2 \sigma_3 q_i}{C_u n_s} \\ - 8.3E(-4)C_c h \varepsilon_a \Delta \varepsilon_a \sigma_3 + 0.03 \sigma_3 + q_i \quad (6)$$

$$\varepsilon_{v_{i+1}} = -\frac{0.1\varepsilon_a}{D_{50} C_c^2 h^2 n_s \Delta \varepsilon_a} + \frac{0.03h}{D_{50} C_c n_s} - \frac{1.6E(-7)e \varepsilon_a \sigma_3 \varepsilon_{v_i}}{C_u^3 C_c^2 h} - \frac{3.6E(-9)h n_s \sigma_3}{C_u C_c^3 e \Delta \varepsilon_a} - \frac{3E(-5)}{C_u C_c \Delta \varepsilon_a^2} \\ + \frac{0.13\varepsilon_a \Delta \varepsilon_a - 1.5E(-4)D_{50} C_u^2 C_c n_s \Delta \varepsilon_a^3 h}{h^2} - 1.6\Delta \varepsilon_a^2 + \varepsilon_{v_i} \\ + \frac{0.5\Delta \varepsilon_a^3 q_i n_s + 271.9h^2 \Delta \varepsilon_a^3 e}{n_s e \sigma_3} - \frac{2.1E(-4)h^3 \varepsilon_{v_i}}{n_s e^2 \Delta \varepsilon_a^2 \sigma_3} \\ + \frac{0.2\varepsilon_{v_i} q_i \Delta \varepsilon_a - 0.3\varepsilon_a^2 \Delta \varepsilon_a - 1.3E(-8)C_u C_c \varepsilon_a^4 q_i}{\varepsilon_a q_i \Delta \varepsilon_a} + 0.05 \quad (7)$$

Figures 2 to 4 show deviator stress-axial strain and volumetric strain-axial strain curves predicted by the EPR models in Equations 6 and 7 against the experimental results for data sets that were used to train the models. A comparison was also made between the predictions

1  
2  
3 of the ANN models suggested by Penumadu and Zhao (1999) and EPR results for the training  
4 data cases. Typical results are presented in Figure 5.

5  
6  
7 After training, the performance of the trained EPR models was verified using 39 sets of  
8 validation data which had not been introduced to EPR during the training phase. This was  
9 done to evaluate the generalisation capabilities of the developed models to unseen cases of  
10 data. Figures 6 to 8 show predictions made by the developed EPR models against the  
11 experimental data which were not previously seen by EPR and were only used to validate the  
12 models. The predicted data sets shown in these figures were obtained from the developed  
13 EPR models using all input parameters directly acquired from experimental test results which  
14 were kept unseen to EPR during the model development process implementing non-  
15 incremental approach. A comparison was also made, in these figures, with the predictions of  
16 the ANN models suggested by Penumadu and Zhao (1999).  
17  
18  
19  
20  
21  
22  
23  
24  
25  
26  
27

28 Comparison of the results and the high COD values for the EPR models (Table 3) indicate the  
29 excellent performance of these models in capturing the underlying relationships between the  
30 contributing parameters and the deviator stress and volumetric strain response of granular  
31 soils and also in generalizing the training to predict the shearing behaviour of these types of  
32 soils under unseen conditions. The results also show that EPR over performs ANN and its  
33 results are a closer match to the actual experimental data.  
34  
35  
36  
37  
38  
39  
40  
41

### 42 **Predicting entire stress paths using the EPR models**

43  
44 The EPR models (Equations 6 and 7) were used to predict the entire stress paths,  
45 incrementally, point by point, in  $q : \varepsilon_a$  and  $\varepsilon_v : \varepsilon_a$  spaces. Results from four different sets of  
46 (testing) data were used to evaluate the ability of the incremental EPR models to predict the  
47 complete behaviour of granular soils during the entire stress paths. The values of average  
48 grain size, coefficients of uniformity and curvature, hardness, shape factor, void ratio and the  
49 confining pressure represented the initial conditions of the soil. Other contributing parameters  
50  
51  
52  
53  
54  
55  
56  
57  
58  
59  
60

including axial strain and the current values of deviator stress and volumetric strain were updated in each incremental step, considering the values from the previous increment and the EPR models outputs in response to an axial strain increment. Figure 9 illustrates the procedure followed for updating of the input parameters and building the entire stress path for the shearing stage of a triaxial test.

At the start of the shearing stage in a conventional triaxial experiment, the values of all parameters were known. Then, for a prescribed increment of axial strain ( $\Delta\varepsilon_a$ ) the values of  $q_{i+1}$ ,  $\varepsilon_{v,i+1}$  were calculated from the EPR models (Equations 6 and 7) respectively). For the next increment, the values of  $\varepsilon_{a,i}$ ,  $q_i$  and  $\varepsilon_{v,i}$  were updated as:

$$q_i = q_{i+1}$$

$$\varepsilon_{v,i} = \varepsilon_{v,i+1}$$

$$\varepsilon_{a,i} = \varepsilon_{a,i} + \Delta\varepsilon_a$$

The incremental procedure was continued until all the points on the curves were predicted and the curves were established. Figures 10 to 13 show the comparisons between the four complete curves predicted using the EPR models following the above incremental procedure and the actual experimental results for 4 data sets. The predicted data sets shown in these figures were obtained from the developed EPR models by using the predictions at increment (j) as input parameters to determine the soil response at increment (j+1). The data for the tests used to demonstrate the capabilities of EPR models to reproduce the entire stress paths had not been introduced to the EPR during the model development process.

The results revealed that the predictions were in a very good agreement with the experimental results. Despite the fact that the entire curves had been predicted point by point and the errors of prediction of the individual points were accumulated in the process, the EPR models were robustly able to predict the complete stress paths. This shows that EPR framework is very

1  
2  
3 effective in modelling the shearing behaviour of granular soils and is able to make reliable  
4  
5 and highly accurate predictions.  
6

### 7 **Sensitivity analysis**

8  
9 A parametric study was carried out on random validation sets of data to evaluate the response  
10  
11 of the models to changes in input parameters. This was done through a basic approach to  
12  
13 sensitivity analysis by fixing all but one input variable to their mean values and varying the  
14  
15 remaining one within the range of its maximum and minimum values available in data.  
16  
17 Results of the sensitivity analysis are shown in Figures 14 to 16. As expected increasing the  
18  
19 average particle size (which indicates that the soil grains are getting coarser) causes the shear  
20  
21 strength of the soil to increase (Figure 14a).  
22  
23

24  
25 Considering the fact that, in case of granular soils, the best way to compact a soil sample is  
26  
27 by vibration rather than compression because of the friction between the coarse grains which  
28  
29 increases under compression and makes it more difficult for the soil grains to move and fill  
30  
31 up the voids, Figure 14b correctly shows the negligible effect of increase in particle size on  
32  
33 volumetric strain under compression in granular soils.  
34

35  
36 Increasing the shape factor parameter shows that angularity of the soil increases resulting in  
37  
38 higher friction and subsequently higher shear strength; however, as the soil grains gets more  
39  
40 angular the possibility of crushing of the angular grains under stress also increases. The  
41  
42 available data suggest that the breakdown stress ( $\sigma_B$ ), beyond which the particle breakdown  
43  
44 occurs, in some types of sand could be as low as  $1 \text{ kN/cm}^2$  (Vesic and Clough 1968).  
45  
46 Deviator stress levels at failure in most test results used in this study were well above this  
47  
48 level exceeding 70000 kPa in some cases, which can be considered as evidence of particle  
49  
50 breakage occurring. Figure 15 shows that, due to the opposing effects of increase in friction  
51  
52 and crushing of angular soil grains under compression, the overall effect of increasing the  
53  
54 shape factor, on shear strength and volumetric strain of granular soils are also negligible.  
55  
56  
57  
58  
59  
60

1  
2  
3 Increasing void ratio causes the shear strength to drop and also the volumetric strain to  
4 increase under shearing. These effects are also correctly predicted by the proposed models  
5  
6  
7 (Figure 16).  
8  
9

## 10 **Discussion and conclusions**

11  
12 Pattern recognition techniques like artificial neural networks have been introduced as an  
13  
14 alternative method of modelling the behaviour of complex systems in recent decades. These  
15  
16 methods have the advantage that they do not require any simplifying assumptions in  
17  
18 developing the models representing the behaviour of systems and can capture the behaviour  
19  
20 materials straight from field measurements and/or experimental results; however, due to their  
21  
22 black box nature, these methods are unable to provide the users with an easy to understand  
23  
24 explicit model providing visible deep insight into the physics of the systems. In this research  
25  
26 work the evolutionary polynomial regression (EPR) was introduced as an alternative  
27  
28 technique with the capability of overcoming some of the issues related to other previously  
29  
30 used artificial intelligence-based modelling techniques aiming at modelling the complex  
31  
32 shearing behaviour of cohesionless soils.  
33  
34  
35

36  
37 In the EPR approach, no pre-processing of the data is required and there is no need for  
38  
39 normalization or scaling of the data. An interesting feature of EPR is in the possibility of  
40  
41 getting more than one model for complex phenomena. The best model is chosen on the basis  
42  
43 of its performances on a testing set which is kept unseen to EPR during the model  
44  
45 development stage.  
46  
47

48  
49 As a result of this study, two models were developed based on EPR to describe the deviator  
50  
51 stress - axial strain and volumetric strain - axial strain behaviour of granular soils. It was  
52  
53 shown that EPR has been able to capture the underlying relationships between various  
54  
55 involved parameters directly from experimental triaxial data and developed models with the  
56  
57  
58  
59  
60

1  
2  
3 ability of predicting the shearing behaviour of granular soils to high accuracy levels. The  
4  
5 EPR models were tested using data that were not used in the training phase of the EPR model  
6  
7 development process; in this way, an unbiased performance indicator was obtained on the  
8  
9 real prediction capability of the models. The results revealed that the EPR-based models were  
10  
11 capable of generalizing the training to predict the behaviour of granular soils under  
12  
13 conditions that have not been previously seen by EPR in the training stage. Through the  
14  
15 comparison of the results it was also shown that the proposed EPR models outperformed  
16  
17 ANN and provided closer predictions to the experimental data cases. An incremental  
18  
19 approach was also taken and was successfully implemented to develop the entire stress paths  
20  
21 for the shearing behaviour of granular soils using developed models with very good accuracy  
22  
23 despite error accumulation. . A parametric study was also conducted to evaluate the effect of  
24  
25 the contributing parameters on the predictions of the proposed EPR models. The results  
26  
27 revealed the consistency of the suggested model predictions, considering the roles of various  
28  
29 contributing parameters, with physical and engineering understandings of the shearing  
30  
31 behaviour of granular soils.  
32  
33

34  
35 However, another interesting feature of EPR is that as more data becomes available, EPR can  
36  
37 be retrained with the latest most comprehensive set of data to create more accurate and  
38  
39 efficient models. The fact that EPR is capable of learning the material behaviour directly  
40  
41 from raw experimental data makes the EPR-based Constitutive Modelling (EPRCM) the  
42  
43 shortest route from the experimental research to the numerical modelling. A trained EPRCM  
44  
45 can be incorporated into a finite element code in the same way as a conventional constitutive  
46  
47 model. This implementation can be done by using either incremental or total stress–strain  
48  
49 strategies. An EPR-based finite element method can be used for solving boundary value  
50  
51 problems in the same way as a conventional finite element method. Examples of  
52  
53  
54  
55  
56  
57  
58  
59  
60

1  
2  
3 implementation of EPR models in finite element analysis can be found in, e.g., Javadi, et al.  
4  
5 (2009) and Javadi, et al. (2012).  
6  
7  
8

## 9 **References**

- 10  
11 Ahangar Asr, Alireza, and Akbar Javadi. 2016. "Air losses in compressed air tunnelling: a  
12 prediction model." *Proceedings of the Institution of Civil Engineers - Engineering*  
13 *and Computational Mechanics*.  
14  
15  
16 Ellis, G W, C Yao, R Zhao, and D Penumadu. 1995. "Stress-strain modeling of sands using  
17 artificial neural networks." *Journal of Geotechnical Engineering, ASCE* 121 (5): 429-  
18 35.  
19  
20  
21 Erzin, Y. 2004. "Strength of Different Anatolian Sands in Wedge Shear, Triaxial Shear, and  
22 Shear Box Tests." *The Middle East Technical University, PhD thesis*.  
23  
24 Ghaboussi, J., D.A. Pecknold, M. Zhang, and R.M. Haj-Ali. 1998. "Autoprogressive training  
25 of neural network constitutive models." *International Journal for Numerical Methods*  
26 *in engineering* 42 (1): 105-126.  
27  
28  
29 Giustolisi, O, and D Savic. 2006. "A symbolic data-driven technique based on evolutionary  
30 polynomial regression." *Journal of Hydroinformatics* 8 (3): 207-222.  
31  
32 Hardin, B O. 1985. "Crushing of soil particles." *Journal of Geotechnical Engineering, ASCE*  
33 111 (10): 1177-92.  
34  
35 Hussain M. S., Javadi A. A., Ahangar-Asr A, Farmani R. 2015. "A surrogate model for  
36 simulation-optimization of aquifer systems." *Journal of Hydrology* 542-554.  
37  
38 Javadi, A A, and M Rezania. 2009. "Applications of artificial intelligence and data mining  
39 techniques in soil modelling." *Geomechanics and Engineering, An International*  
40 *Journal* 1 (1): 53-74.  
41  
42  
43 Javadi, Akbar A, Asaad Faramarzi, and Alireza Ahangar-Asr. 2012. "Analysis of behaviour  
44 of soils under cyclic loading using EPR-based finite element method." *Finite*  
45 *Elements in Analysis and Design* 53-65.  
46  
47  
48 Javadi, Akbar A, Moura Mehravar, Asaad Faramarzi, and Alireza Ahangar-Asr. 2009. "An  
49 Artificial Intelligence Based Finite Element Method." *Transactions on Computers*  
50 *and Intelligent Systems* 1-7.  
51  
52  
53 Lee, K L, and H B Seed. 1967. "Drained strength characteristics of sands." *J. Soil Mech. and*  
54 *Found. Div., ASCE* 93 (6): 117-141.  
55  
56  
57  
58  
59  
60



- 1  
2  
3 Lee, K L, H B Seed, and P Dunlop. 1967. "Effect of moisture on the strength of clean sand."  
4 *J. Soil Mech. and Found. Div., ASCE* 93 (6): 17-40.  
5  
6 Leslie, D D. 1975. "Shear strength of rock fill." *Physical Properties Engrg. Study No. 526,*  
7 *U.S. Army Corps of Engrs., Sausalito, CA.*  
8  
9 Lo, K Y, and M Roy. 1973. "Response of particulate materials at high-pressures." *Soils and*  
10 *Foundations, JSSMFE* 13 (1): 61-76.  
11  
12 Marachi, N D, C K Chan, H B Seed, and J M Duncan. 1969. "Strength and deformation  
13 characteristics of rockfill materials." *Report No. TE-69-5, Dept. of Civil Engrg., Univ.*  
14 *Of California, Berkeley, CA.*  
15  
16 Miura, N, and S O-Hara. 1979. "Particle crushing of a decomposed granite soil under shear."  
17 *Soils and Foundations, JSSMFE* 19 (3): 1-14.  
18  
19 Miura, N, and T Yamanouchi. 1975. "Effect of water on the behavior of quartz-rich sand  
20 under high stresses." *Soils and Foundations, JSSMFE* 15 (4): 23-34.  
21  
22 Penumadu, D, and R Zhao. 1999. "Triaxial compression behavior of sand and gravel using  
23 arti©cial neural networks (ANN)." *Computers and Geotechnics* 24: 207-230.  
24  
25 Ponce, V M, and J M Bell. 1971. "Shear strength of sand at extremely low pressures." *J. Soil*  
26 *Mech. and Found.Div., ASCE* 97 (4): 625-639.  
27  
28 Ramamurthy, T, V K Kanitar, and K Prakash. 1974. "Behavior of coarse-grained soils under  
29 high stresses." *Indian Geotech. J.* 4 (1): 39-63.  
30  
31 Raymond, G P, and J R Davies. 1978. "Triaxial tests on dolomite railroad ballast." *J.*  
32 *Geotech. Engrg., ASCE* 104 (6): 737-751.  
33  
34 Raymond, G P, and V A Diyaljee. 1979. "Railroad ballast load ranking classification." *J.*  
35 *Geotech. Engrg., ASCE* 105 (10): 1133-1153.  
36  
37 Rowe, C W, and L Barden. 1964. "Importance of free ends in triaxial testing." *Journal of the*  
38 *Soil Mechanics and Foundations Division, ASCE* 90 (1): 1-28.  
39  
40 Vesic, Aleksandar S, and G Wayne Clough. 1968. "Behaviour of Granular Materials Under  
41 High Stresses." *Soil Mechanics and Foundations Division* 661-688.  
42  
43 Wu, T H. 1957. "Relative density and shear strength of sands." *J. Soil Mech. and Found.*  
44 *Div., ASCE* 83 (1): 1161:1-23.  
45  
46  
47  
48  
49  
50  
51  
52  
53  
54  
55  
56  
57  
58  
59  
60

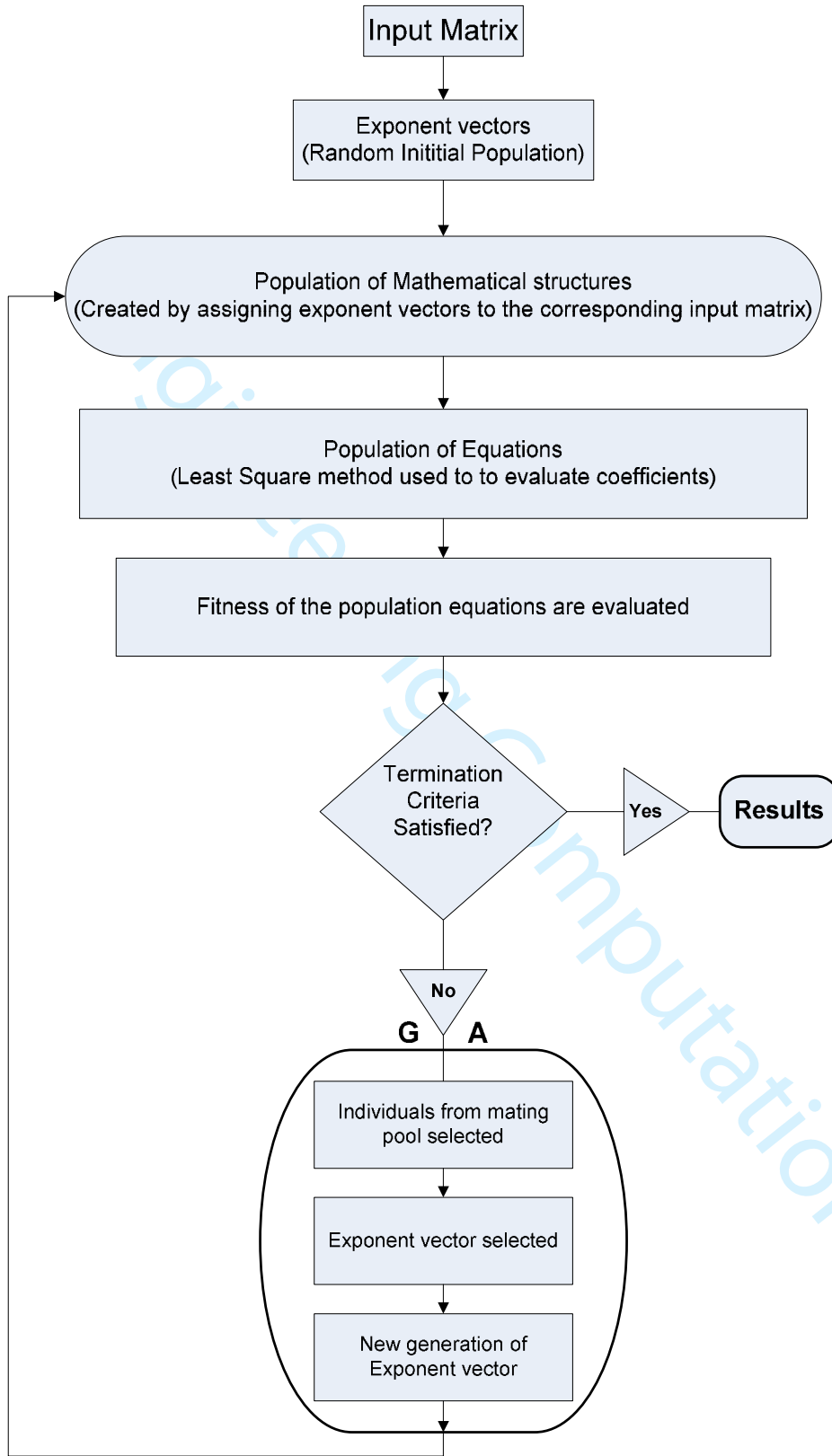
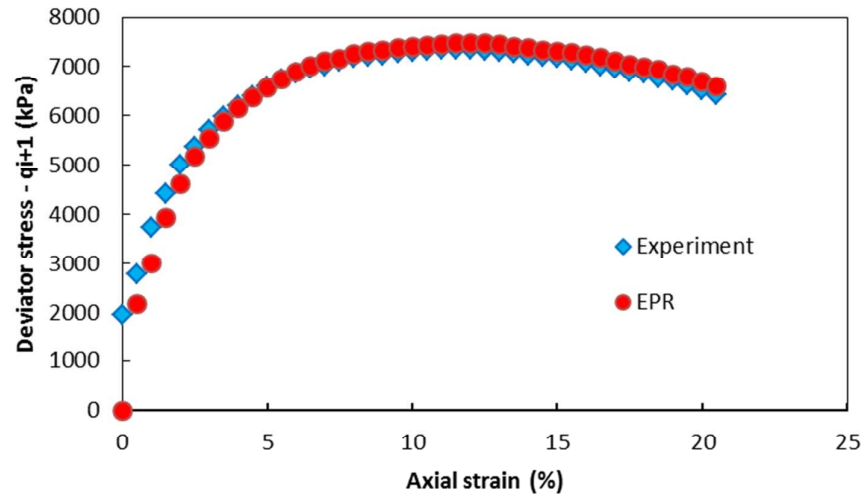
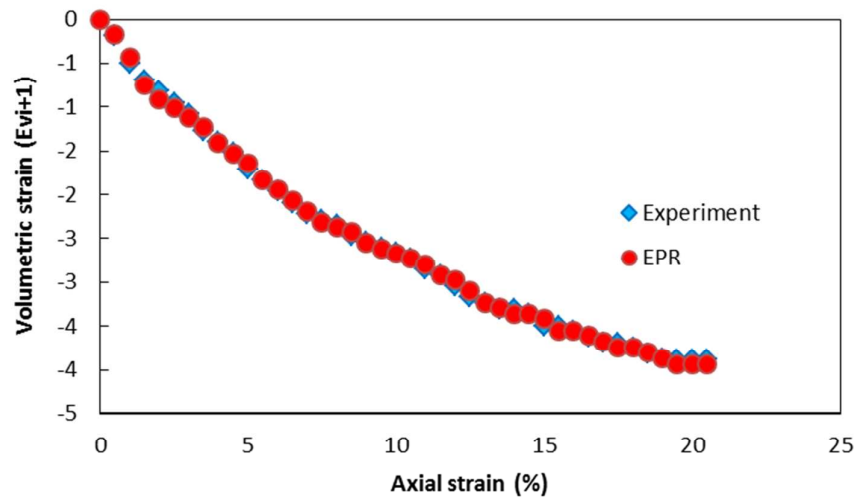


Figure 1: Flow diagram for EPR procedure



(a)



(b)

**Figure 2:** (a) Deviator stress-axial strain and (b) volumetric strain-axial strain curves predicted by the EPR models compared to experimental data ( $\sigma_3 = 2932 \text{ kPa}$ ) – training data case (Experimental data from Lee and Seed (1967))

1  
2  
3  
4  
5  
6  
7  
8  
9  
10  
11  
12  
13  
14  
15  
16  
17  
18  
19  
20  
21  
22  
23  
24  
25  
26  
27  
28  
29  
30  
31  
32  
33  
34  
35  
36  
37  
38  
39  
40  
41  
42  
43  
44  
45  
46  
47  
48  
49  
50  
51  
52  
53  
54  
55  
56  
57  
58  
59  
60

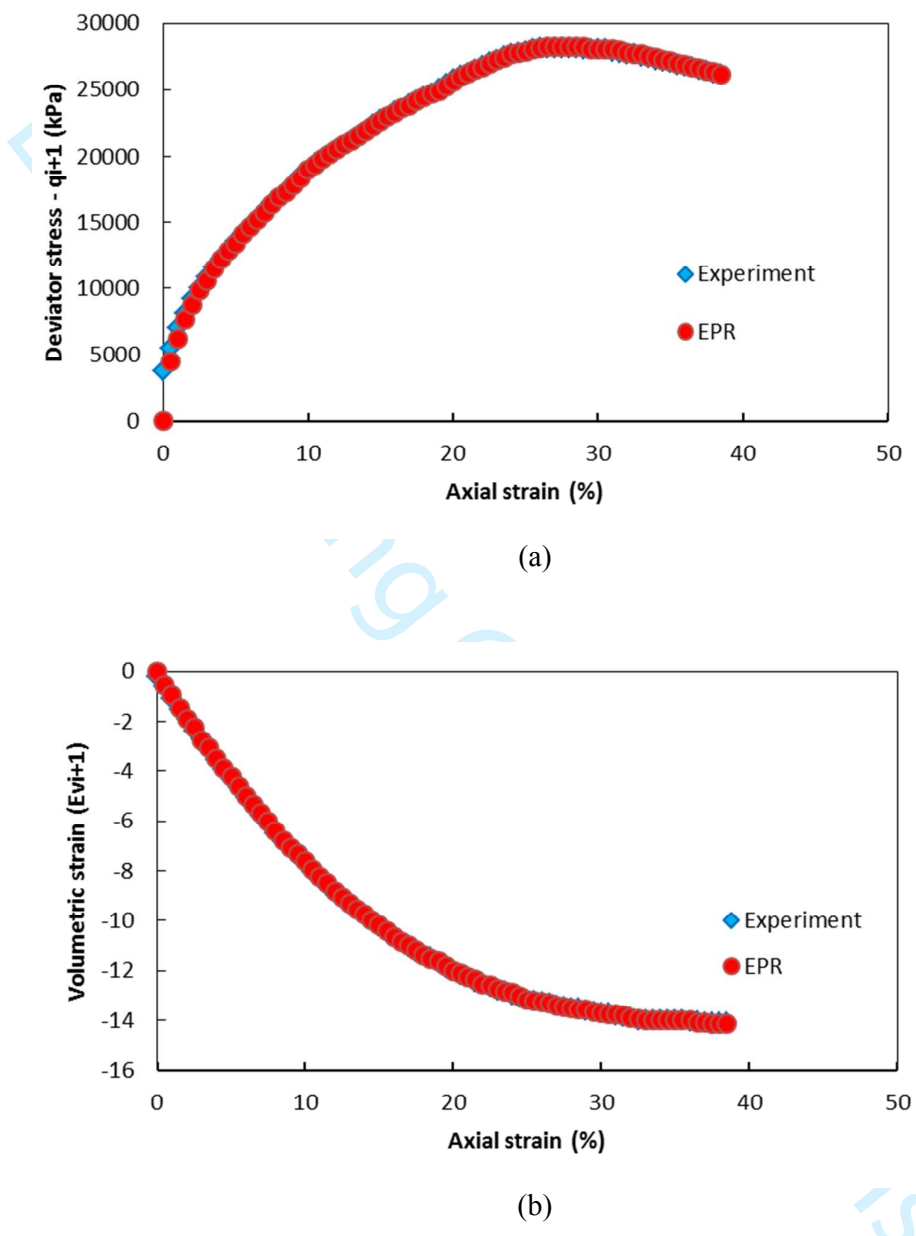
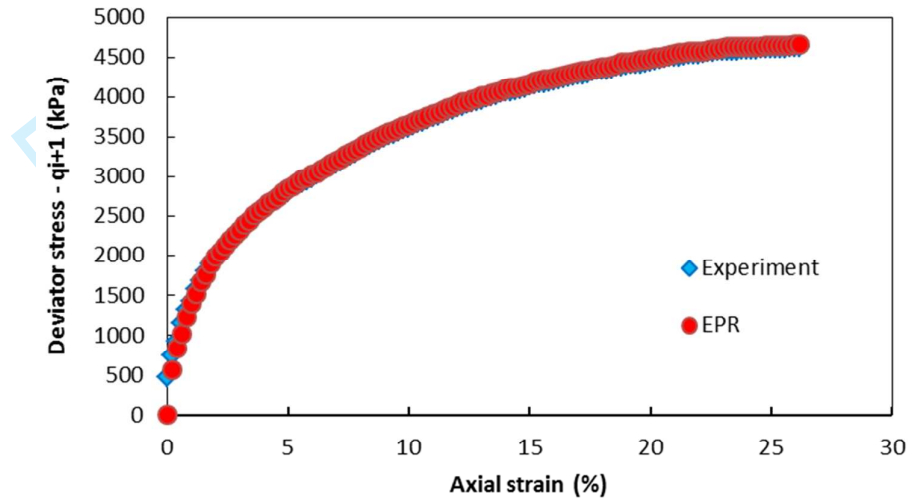
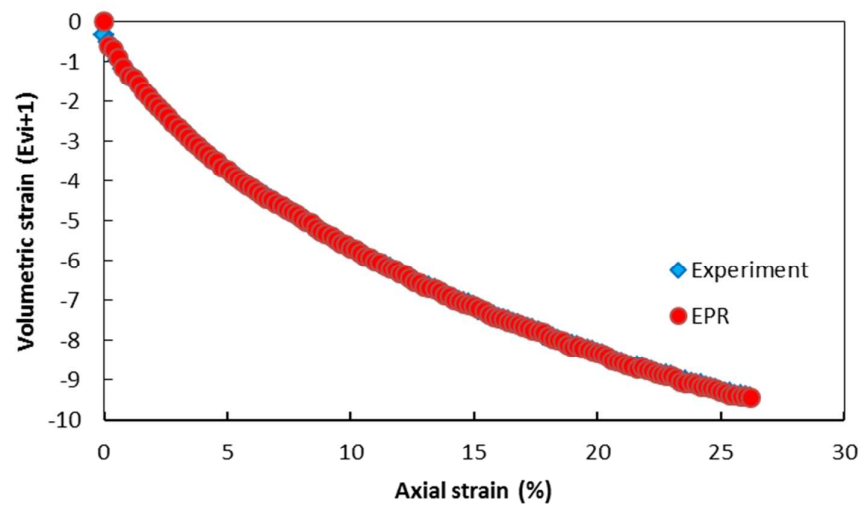


**Figure 3:** (a) Deviator stress-axial strain and (b) volumetric strain-axial strain curves predicted by the EPR models compared to experimental data ( $\sigma_3 = 11767 \text{ kPa}$ ) – training data case (Experimental data from Lee and Seed (1967))



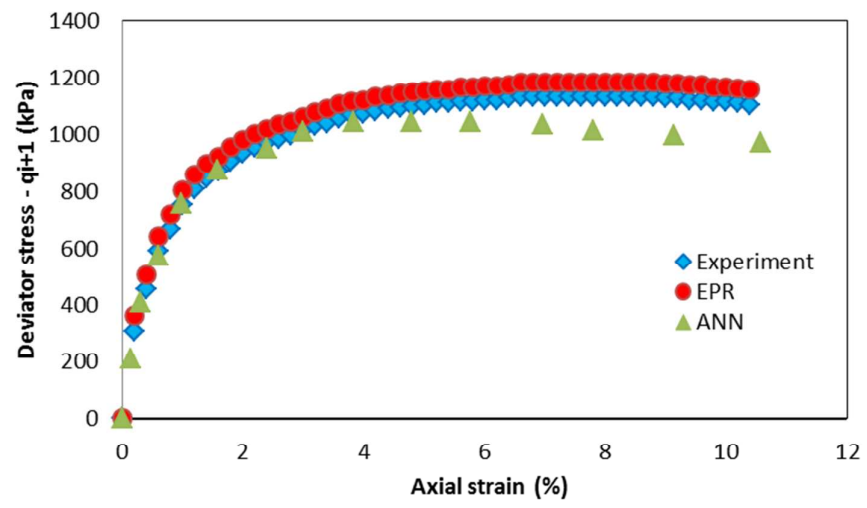
(a)



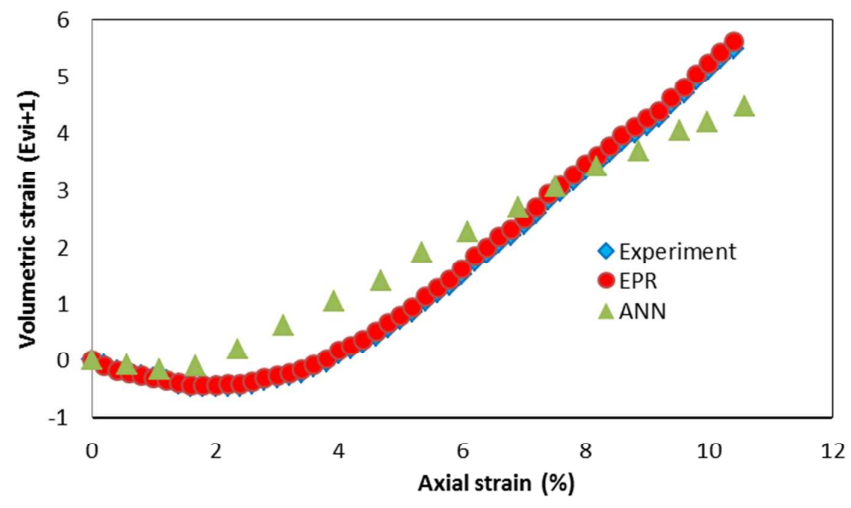
(b)

**Figure 4:** (a) Deviator stress-axial strain and (b) volumetric strain-axial strain curves predicted by the EPR models compared to experimental data ( $\sigma_3 = 1961 \text{ kPa}$ ) – training data case (Experimental data from Lee and Seed (1967))

1  
2  
3  
4  
5  
6  
7  
8  
9  
10  
11  
12  
13  
14  
15  
16  
17  
18  
19  
20  
21  
22  
23  
24  
25  
26  
27  
28  
29  
30  
31  
32  
33  
34  
35  
36  
37  
38  
39  
40  
41  
42  
43  
44  
45  
46  
47  
48  
49  
50  
51  
52  
53  
54  
55  
56  
57  
58  
59  
60

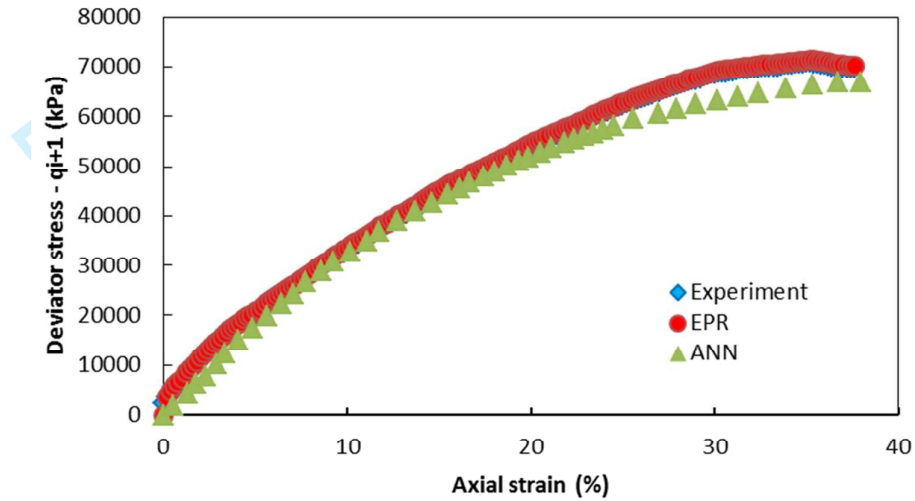


(a)

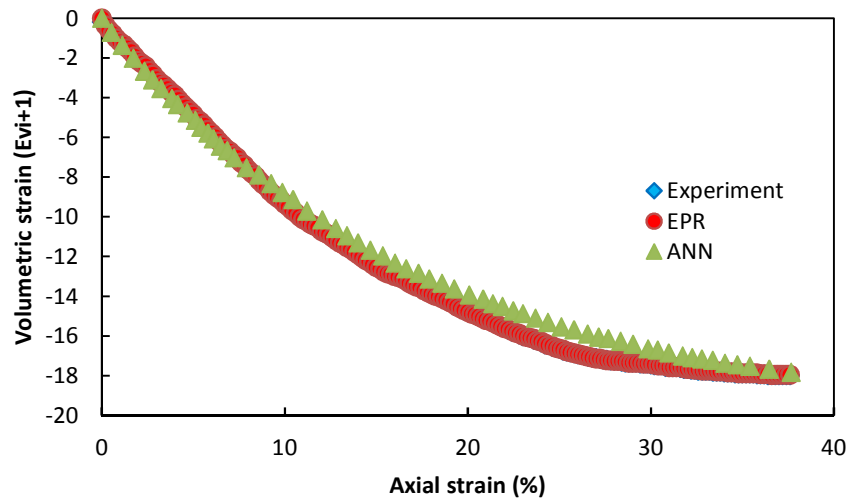


(b)

**Figure 5:** (a) Deviator stress-axial strain and (b) volumetric strain-axial strain curves predicted by the EPR models compared to experimental data and ANN model predictions ( $\sigma_3 = 275 \text{ kPa}$ ) – training data case (Experimental data from Wu (1957))



(a)



(b)

**Figure 6:** (a) Deviator stress-axial strain and (b) volumetric strain-axial strain curves predicted by the EPR models compared to experimental data and ANN model predictions ( $\sigma_3 = 11767$  kPa) – testing data case (Experimental data from Lee and Seed (1967))

1  
2  
3  
4  
5  
6  
7  
8  
9  
10  
11  
12  
13  
14  
15  
16  
17  
18  
19  
20  
21  
22  
23  
24  
25  
26  
27  
28  
29  
30  
31  
32  
33  
34  
35  
36  
37  
38  
39  
40  
41  
42  
43  
44  
45  
46  
47  
48  
49  
50  
51  
52  
53  
54  
55  
56  
57  
58  
59  
60

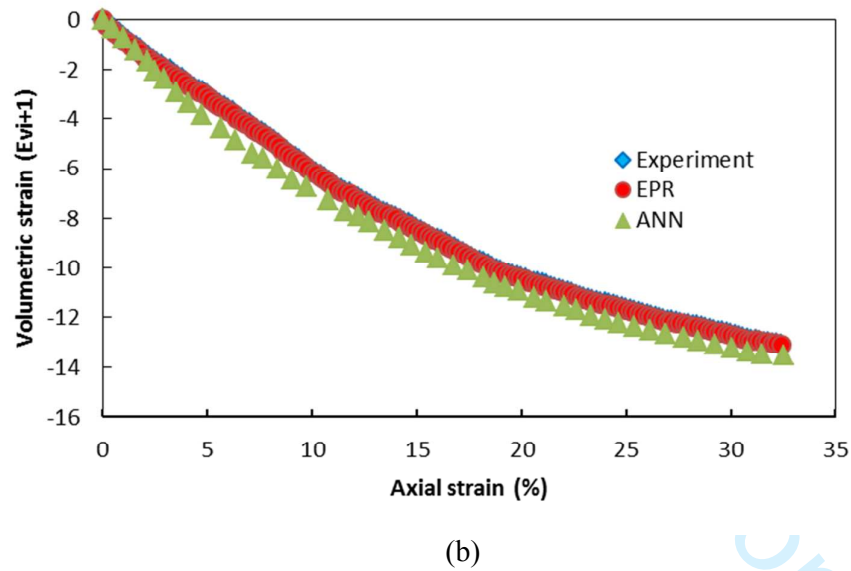
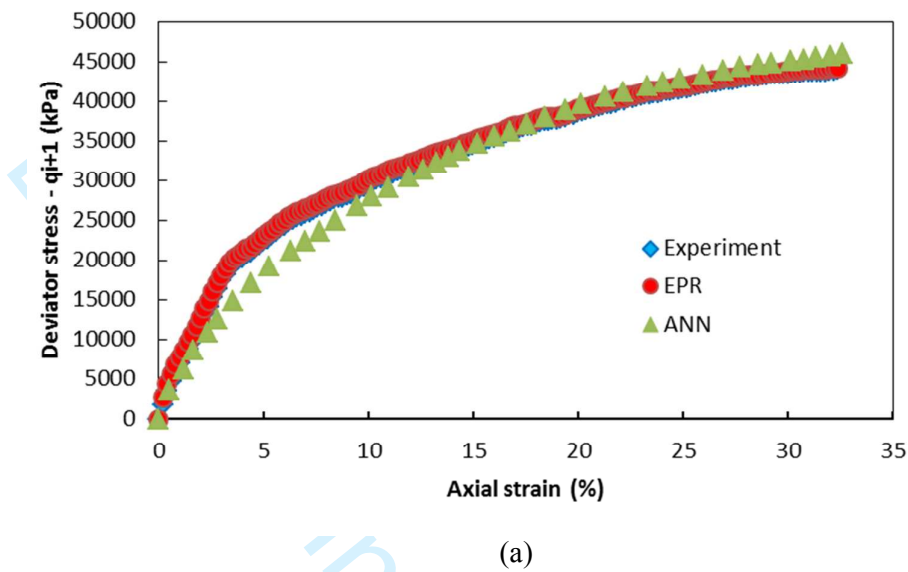
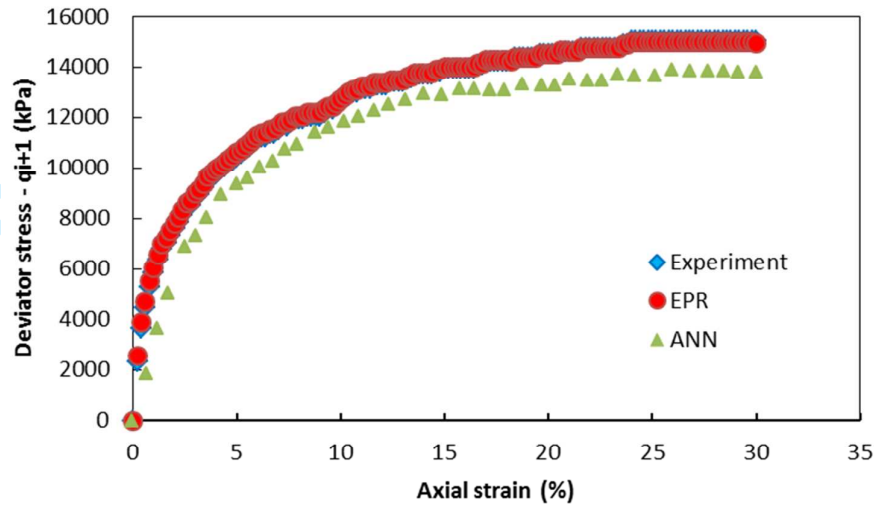
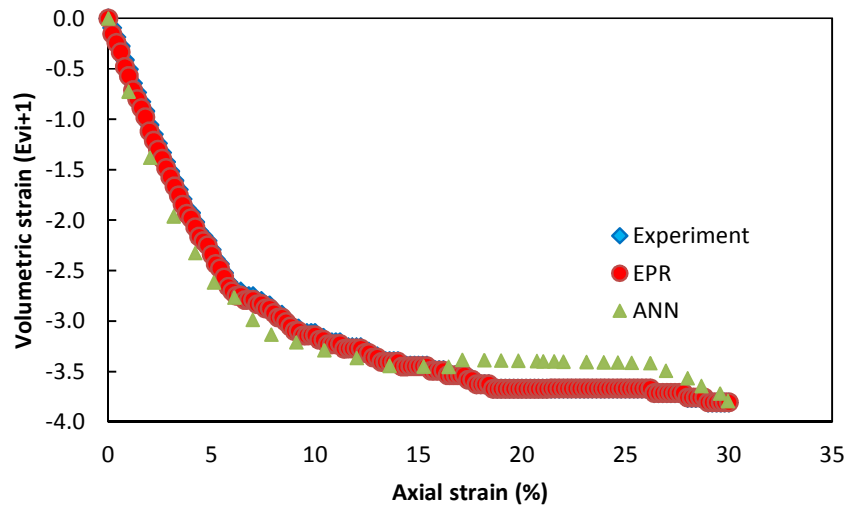


**Figure 7:** (a) Deviator stress-axial strain and (b) volumetric strain-axial strain curves predicted by the EPR models compared to experimental data and ANN model predictions ( $\sigma_3 = 19613 \text{ kPa}$ ) – testing data case (Experimental data from Miura and Yamanouchi (1975))





(a)



(b)

**Figure 8:** (a) Deviator stress-axial strain and (b) volumetric strain-axial strain curves predicted by the EPR models compared to experimental data and ANN model predictions ( $\sigma_3 = 5515 \text{ kPa}$ ) – testing data case (Experimental data from Lo and Roy (1973))

1  
2  
3  
4  
5  
6  
7  
8  
9  
10  
11  
12  
13  
14  
15  
16  
17  
18  
19  
20  
21  
22  
23  
24  
25  
26  
27  
28  
29  
30  
31  
32  
33  
34  
35  
36  
37  
38  
39  
40  
41  
42  
43  
44  
45  
46  
47  
48  
49  
50  
51  
52  
53  
54  
55  
56  
57  
58  
59  
60

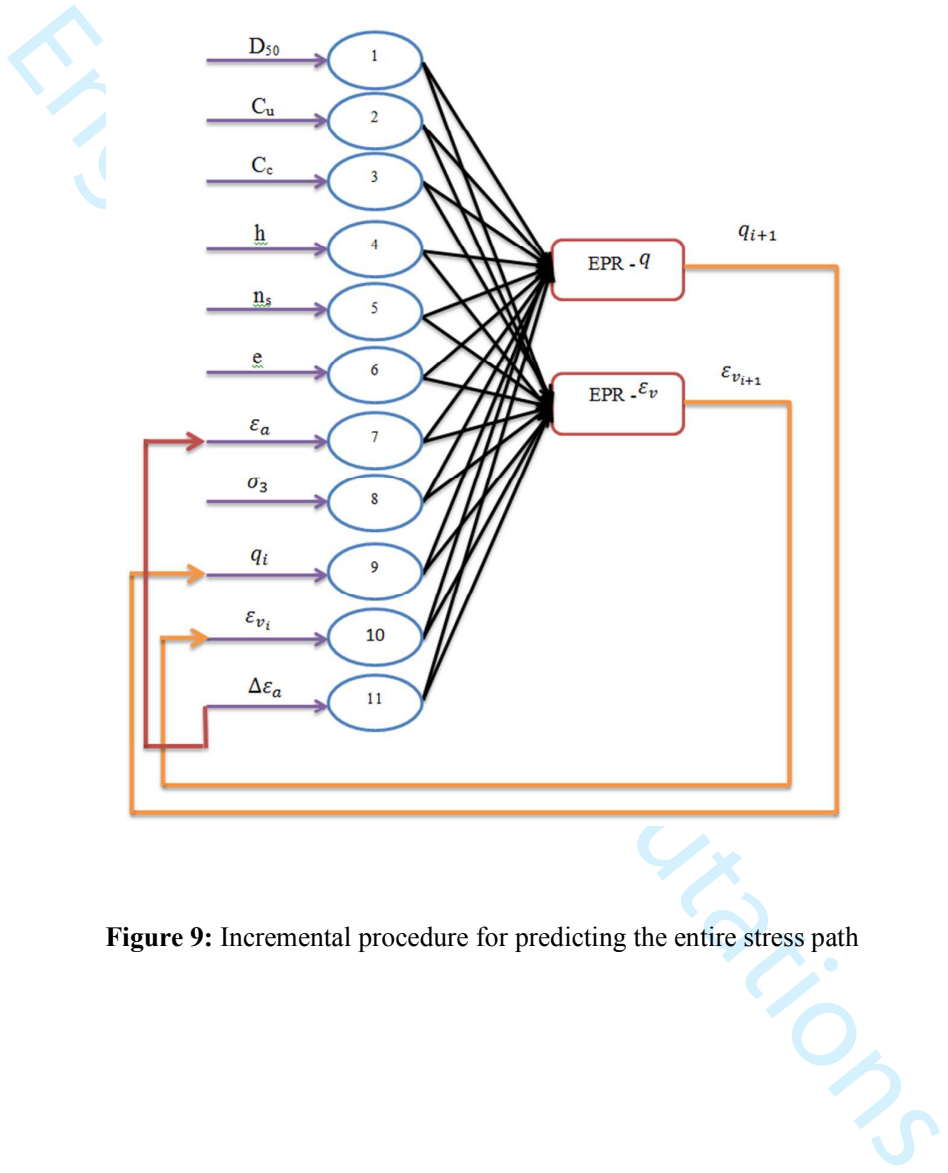
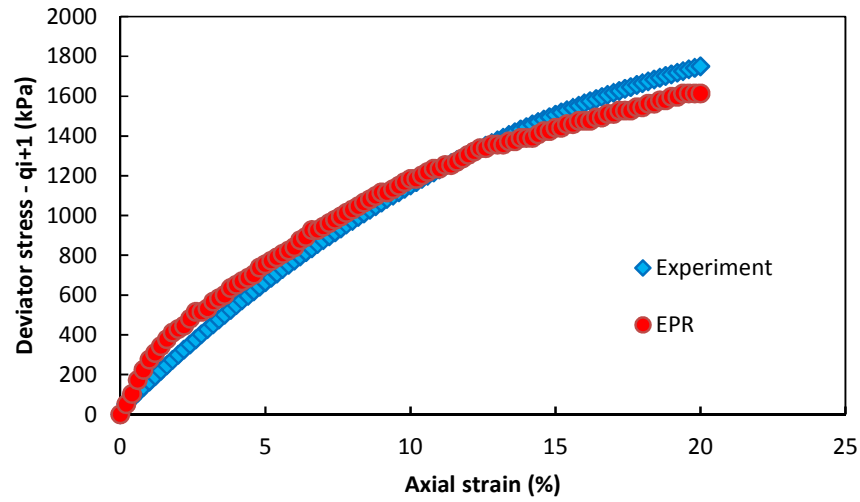
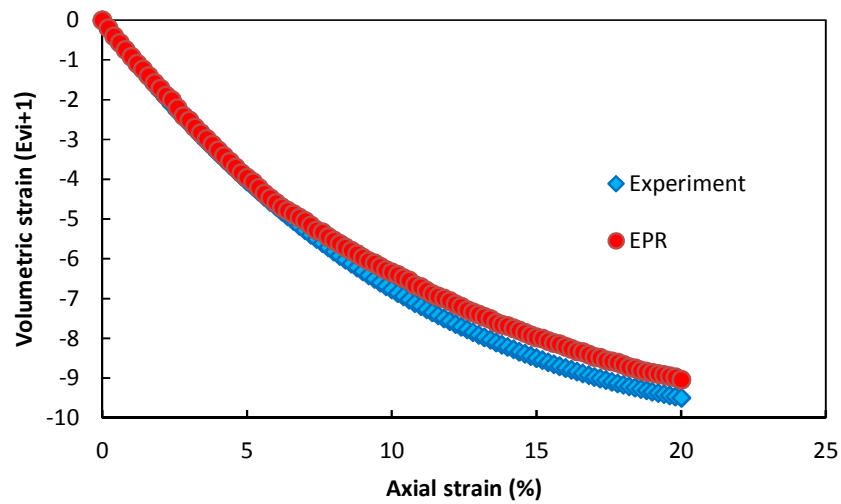


Figure 9: Incremental procedure for predicting the entire stress path



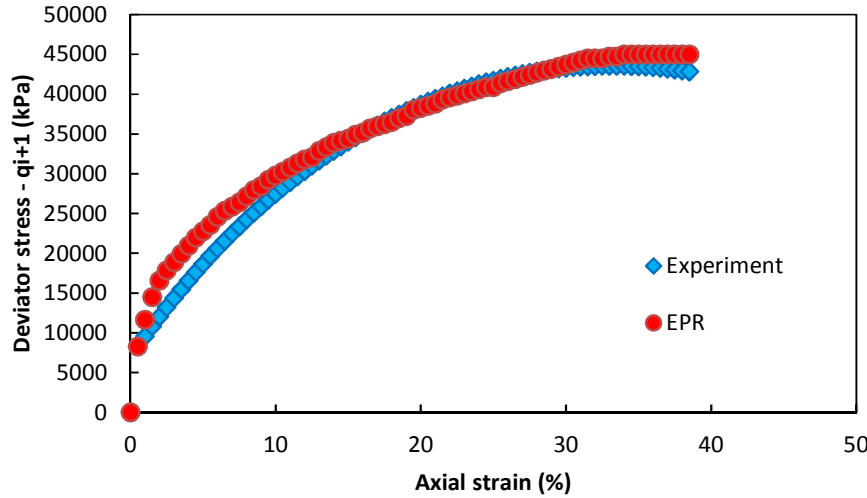
(a)



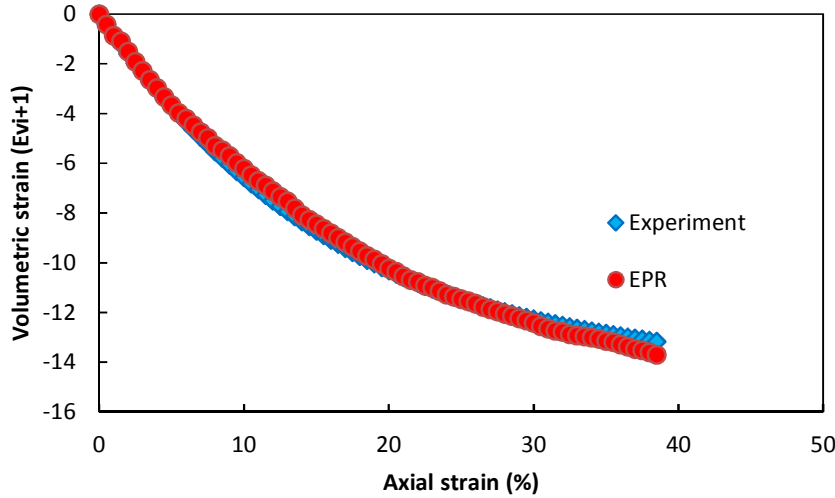
(b)

**Figure 10:** (a) Deviator stress-axial strain and (b) volumetric strain-axial strain curves predicted by the EPR models compared to experimental data ( $\sigma_3 = 413 \text{ kPa}$ ) – testing data case, entire stress path prediction (Experimental data from Leslie (1975))

1  
2  
3  
4  
5  
6  
7  
8  
9  
10  
11  
12  
13  
14  
15  
16  
17  
18  
19  
20  
21  
22  
23  
24  
25  
26  
27  
28  
29  
30  
31  
32  
33  
34  
35  
36  
37  
38  
39  
40  
41  
42  
43  
44  
45  
46  
47  
48  
49  
50  
51  
52  
53  
54  
55  
56  
57  
58  
59  
60

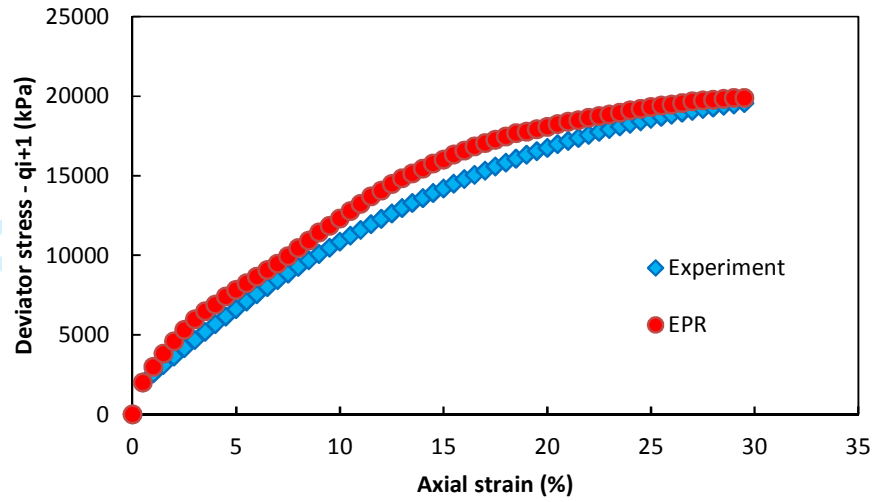


(a)

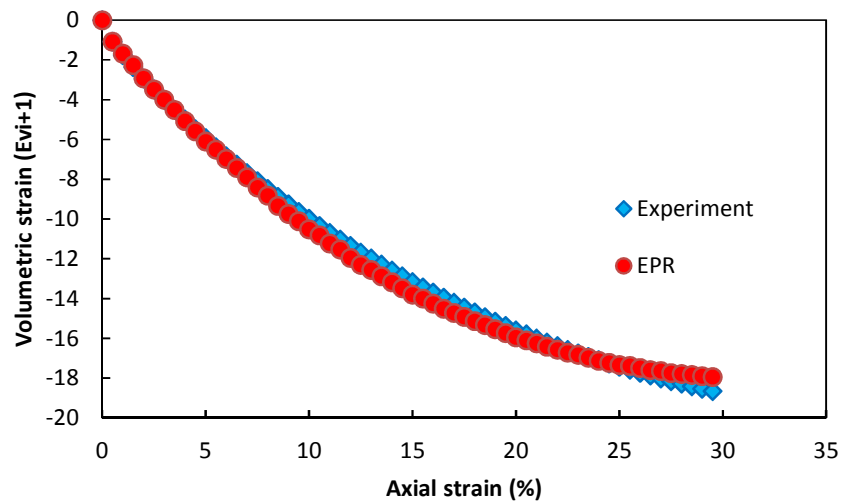


(b)

**Figure 11:** (a) Deviator stress-axial strain and (b) volumetric strain-axial strain curves predicted by the EPR models compared to experimental data ( $\sigma_3 = 19613 \text{ kPa}$ ) – testing data case, entire stress path prediction (Experimental data from Miura and Yamanouchi (1975))



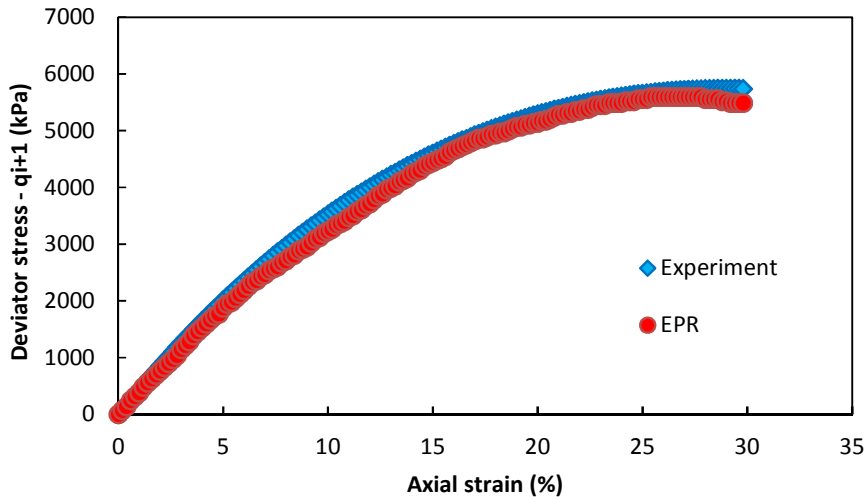
(a)



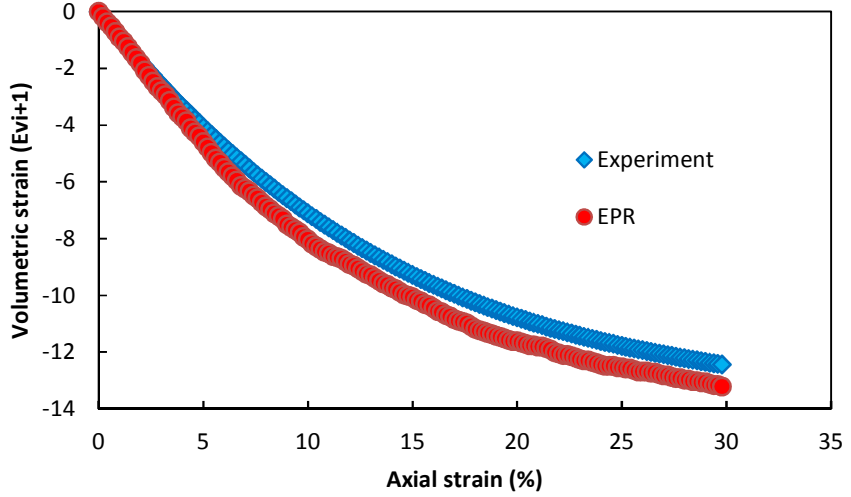
(b)

**Figure 12:** (a) Deviator stress-axial strain and (b) volumetric strain-axial strain curves predicted by the EPR models compared to experimental data ( $\sigma_3 = 8276$  kPa) – testing data case, entire stress path prediction (Experimental data from Ramamurthy, Kanitar and Prakash (1974))

1  
2  
3  
4  
5  
6  
7  
8  
9  
10  
11  
12  
13  
14  
15  
16  
17  
18  
19  
20  
21  
22  
23  
24  
25  
26  
27  
28  
29  
30  
31  
32  
33  
34  
35  
36  
37  
38  
39  
40  
41  
42  
43  
44  
45  
46  
47  
48  
49  
50  
51  
52  
53  
54  
55  
56  
57  
58  
59  
60

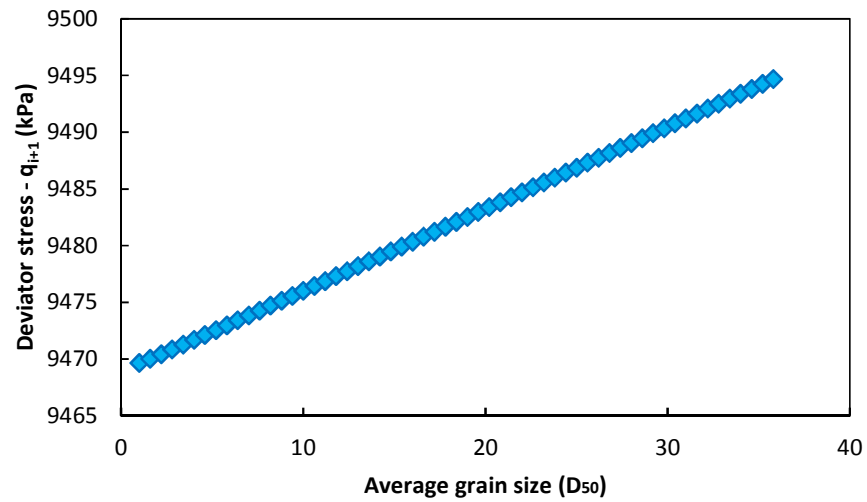


(a)

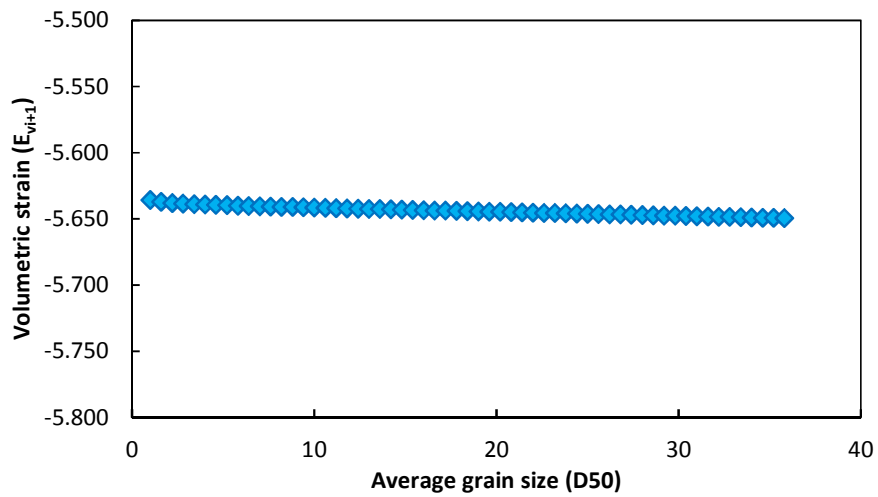


(b)

**Figure 13:** (a) Deviator stress-axial strain and (b) volumetric strain-axial strain curves predicted by the EPR models compared to experimental data ( $\sigma_3 = 2068 \text{ kPa}$ ) – testing data case, entire stress path prediction (Experimental data from Leslie (1975))



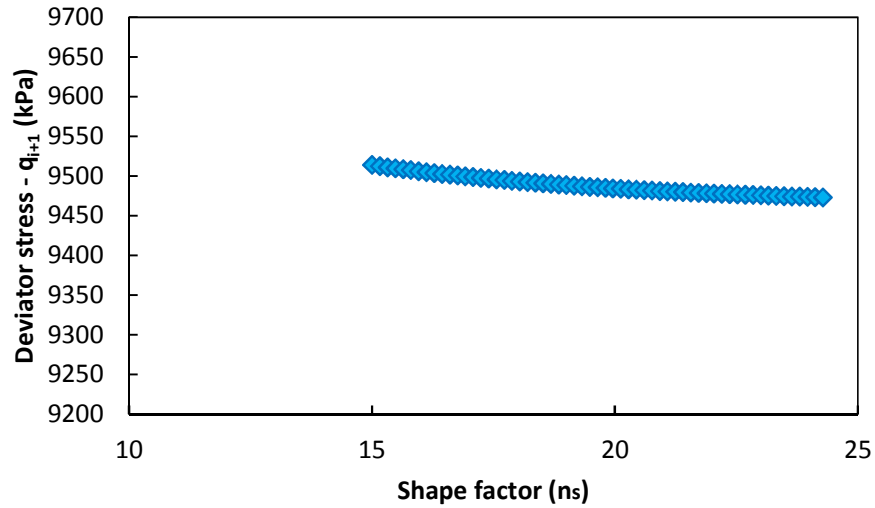
(a)



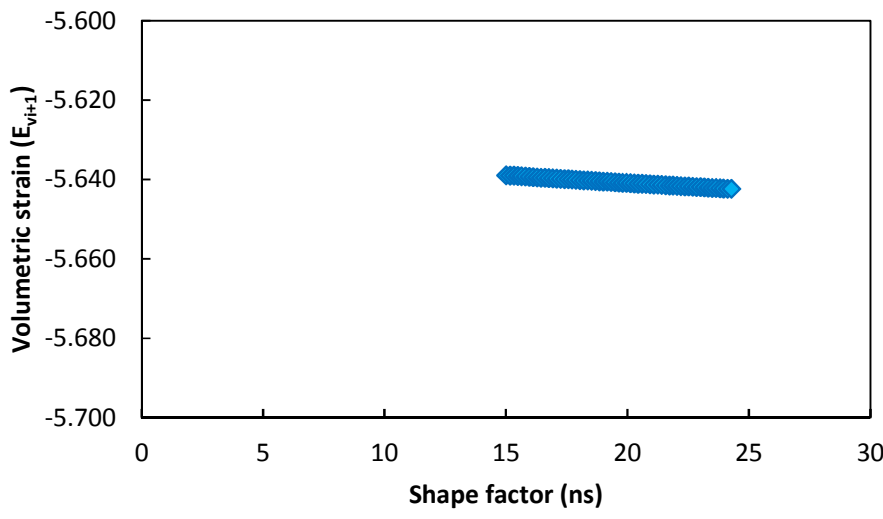
(b)

**Figure 14:** Sensitivity analysis results considering the effect of average grain size  $D_{50}$  on EPR model predictions for (a) deviator stress and (b) volumetric strain.

1  
2  
3  
4  
5  
6  
7  
8  
9  
10  
11  
12  
13  
14  
15  
16  
17  
18  
19  
20  
21  
22  
23  
24  
25  
26  
27  
28  
29  
30  
31  
32  
33  
34  
35  
36  
37  
38  
39  
40  
41  
42  
43  
44  
45  
46  
47  
48  
49  
50  
51  
52  
53  
54  
55  
56  
57  
58  
59  
60



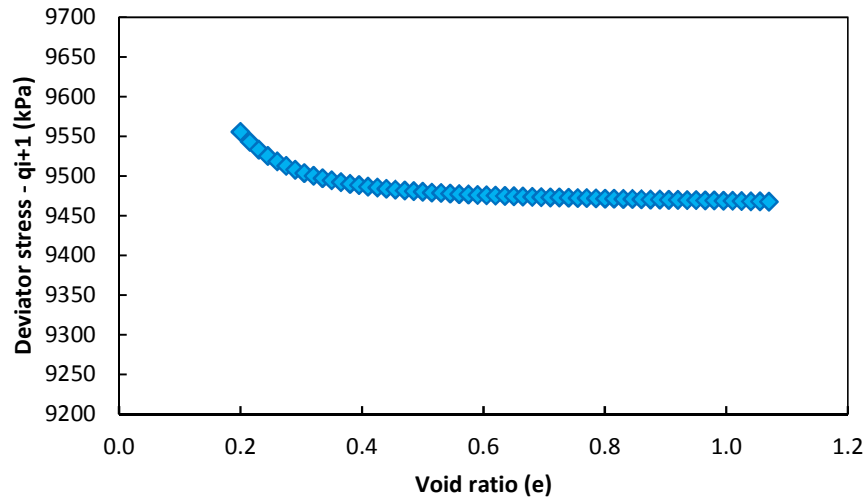
(a)



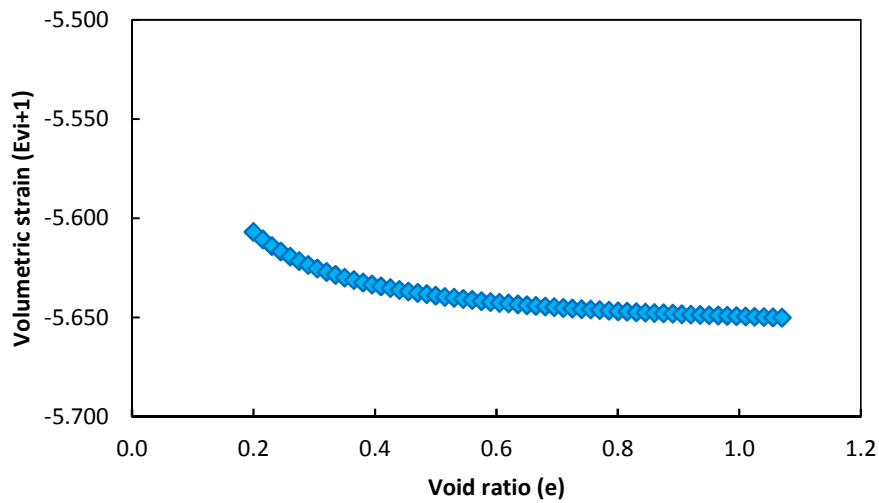
(b)

**Figure 15:** Sensitivity analysis results considering the effect of shape factor ( $n_s$ ) parameter on EPR model predictions for (a) deviator stress and (b) volumetric strain.





(a)



(b)

**Figure 16:** Sensitivity analysis results considering the effect of void ratio parameter ( $e$ ) on EPR model predictions for (a) deviator stress and (b) volumetric strain.

**Table 1:** Data sources used to create the database

<b>Reference</b>	<b>Experimental soil description</b>
Lee and Seed (1967)	Sacramento river sand
Lee, Seed and Dunlop (1967)	Antioch sand
Leslie (1975)	Napa basalt New Hogan metavolcanic Carters Dam quartzite Cougar basalt Sonora dolomite Laurel sandstone Buchanan weathered granite
Lo and Roy (1973)	Back mine quartz sand St. Marc limestone sand Aluminum oxide sand
Marachi et al (1969)	Pyramid dam material Napa basalt
Miura and Yamanouchi (1975)	Toyoura sand
Miura and O-Hara (1979)	Ube decomposed granite
Ponce and Bell (1971)	Quartz sand
Ramamurthy et al (1974)	Badarpur sand
Raymond and Davies (1978)	Coteau dolomite Kenora granite Nouvelle igneous Sudburg slag
Raymond and Diyaljee (1979)	Grenville marble Kimberly float St. Isodore limestone Brandon gravel St. Bruno shale
Wu (1957)	Fluvioglacial sand
Erzin (2004)	Anatolian sands

**Table 2:** Parameters involved in the developed EPR models\*

Contributing parameters	Model output
$D_{50}, C_u, C_c, h, n_s, e, \sigma_3$	$q_{i+1}$
$\varepsilon_a, \Delta\varepsilon_a, q_i, \varepsilon_{v,i}$	$\varepsilon_{v,i+1}$

\*  $D_{50}$  (mm) = average grain size,  $C_u$  = coefficient of uniformity,  $C_c$  = coefficient of curvature;  $h$  = hardness of the mineral;  $\varepsilon_a$  = axial strain;  $n_s$  = shape factor;  $\varepsilon_v$  = volumetric strain;  $q$  = deviator stress;  $\Delta\varepsilon_a$  = axial strain increment;  $e$  = void ratio;  $\sigma_3$  = effective confining pressure.

**Table 3:** COD values for EPR models

Equation	COD values for training (%)	COD values for testing (%)
Deviator stress (Equation 6)	99.99	99.98
Volumetric strain (Equation 7)	99.99	99.99